J. Fluid Mech. (1995), *vol.* 286, *pp.* 257–276

Chaotic mode competition in the shape oscillations of pulsating bubbles

By D. ZARDI AND G. SEMINARA

Istituto di Idraulica, Facoltà di Ingegneria, Università di Genova,
Via Montallegro 1, 16145 Genova, Italy

(Received 7 June 1994)

A possible mechanism for the occurrence of the phenomenon of *erratic drift* of bubbles in liquids subjected to acoustic waves was proposed by Benjamin & Ellis (1990) who showed that nonlinear interactions between adjacent perturbation modes expressed in terms of spherical harmonics of any order may lead to the excitation of mode 1 which is equivalent to a displacement of the bubble centroid. We show that indeed such a mechanism can give rise to a chaotic process at least under the conditions experimentally investigated by Benjamin & Ellis (1990). In fact we examine the case in which the angular frequency ω of the incident wave is sufficiently close to both the natural frequency of mode $n+1$ (ω_{n+1}) and twice the natural frequency of mode n ($2\omega_n$) thus exciting simultaneously a subharmonic mode n and a synchronous mode $n+1$. The value of n is set equal to 3 in accordance with Benjamin & Ellis' (1990) observation. A classical multiple scale analysis allows us to follow the development of these perturbations in the weakly nonlinear regime to find an autonomous system of quadratically coupled nonlinear differential equations governing the evolution of the amplitudes of the perturbations on a slow time scale. As obtained by Gu & Sethna (1987) for the Faraday resonance problem, we find both regular and chaotic solutions of the above system. Chaos is found to develop for large enough values of the amplitude of the acoustic excitation within some region in the parameter space and is reached through a period-doubling sequence displaying the typical characteristics of Feigenbaum scenario.

1. Introduction

The dynamics of gas bubbles in a liquid subjected to an acoustic wave has been widely explored both in the context of technical problems (like detection and prevention of cavitation, underwater acoustic sensing, effects of ultrasound on microcavities in physiologic liquids, microchemistry), and to investigate some interesting theoretical questions arising from peculiar behaviour displayed by bubbles, like the so-called effect of 'erratic drift', a phenomenon of chaotic self-propulsion experimentally observed and reported by various authors (Gaines 1932; Kornfeld & Suvorov 1944; Strasberg & Benjamin 1958; Benjamin & Ellis 1990).

Early research work on radially oscillating bubbles as possible sources of underwater sound date back to Rayleigh (1917), who first stated the well-known nonlinear equation governing the oscillations of the bubble radius. Indeed a pure radial oscillation of the bubble surface (*breathing mode*) is obviously the simplest kind of motion one can expect to be set up when the initial/boundary conditions bear spherical symmetry. This may occur whenever the sound wavelength is much greater than the

mean bubble radius, so that the sound field is 'felt' by the bubble as almost uniform in space and pulsating in time.

Shape oscillations are also possible, and can be analysed in terms of a superposition of spherical harmonics each having its own natural frequency, say ω_n.

A linear stability analysis of the basic radial motion was performed by Plesset & Mitchell (1950) who found that the governing equation for the nth mode perturbation may be reduced to a Hill equation which, for small wave amplitudes, reduces to a Mathieu equation (Eller & Crum 1970; Benjamin & Strasberg 1958; Hsieh & Plesset 1961).

The well-known results about the stability of solutions of the Mathieu equation can then be used to show that under suitable conditions n—th components of bubble surface distortion characterized by frequency half that of the incident wave (ω) (subharmonic response) or by the same frequency (synchronous) or by a multiple frequency (ultraharmonic) may grow depending on how close the value of ω is to $2\omega_n$, ω_n, $\frac{1}{2}\omega_n$ or a smaller integral fraction of ω_n.

Experiments (Elder 1959; Gould 1966) confirm that such surface oscillations arise as a bifurcation from the basic radial motion, occurring in relatively low-viscosity liquids as the amplitude of the acoustic field exceeds a threshold dependent on the relevant parameters of the problem. Further increase of the wave amplitude may lead to successive bifurcations and eventually to a chaotic surface agitation.

The weakly nonlinear development of an unstable mode was investigated by Hall & Seminara (1980), both in the subharmonic and in the synchronous cases. Various types of bifurcations (supercritical, subcritical, transcritical and secondary) were shown to occur under various conditions.

The investigation of finite-amplitude oscillations allowing for nonlinear interactions between different modes seems capable of explaining the physical mechanisms underlying some experimentally observed effects. In this direction, let us recall results obtained by Longuet-Higgins (1989*a*, *b*), who has shown how the emission of monopole radiation of sound can be due to the interaction of distortion modes at second order. Moreover Benjamin & Ellis (1990), developing ideas previously outlined by Saffman (1967), have shown that nonlinear interactions between two adjacent modes (say n and $n+1$) can give rise to the excitation of a mode 1 component of the velocity potential of the surrounding fluid. They pointed out that a Legendre polynomial of order 1 describes a perturbation of the sphere which corresponds to a translation of the bubble. Its excitation then provides a possible mechanism for the above-mentioned phenomenon of *'erratic drift'*.

A great deal of interest has been recently been devoted to parametrically excited mode interactions in surface waves, from which the occurrence of chaotic behaviour is shown to be possible when some relevant parameters attain critical values, and in particular when conditions of external or internal resonance are met (Miles 1984; Ciliberto & Gollub 1985; Holmes 1986; Gu & Sethna 1987; Simonelli & Gollub 1989; Feng & Sethna 1989; Kambe & Umeki 1990). The strict analogy between the hydrodynamical problems of surface waves in oscillating containers and acoustically induced bubble oscillations (Lamb 1932, Art.275; Benjamin 1987; Longuet-Higgins 1989*a*) suggests that one may gain further understanding of the latter processes using some tools developed in the former context. Mei & Zhou (1991) have studied the interaction between the breathing mode and one or two distortional modes requiring both that the former be at resonance with the externally forcing wave and that an internal resonance condition be met by interacting modes. More recently Feng & Leal (1994) have examined the case when the frequency ratio of the volume mode and one

shape mode is assumed to be close to two-to-one, detecting various bifurcation paths. Both of these works however allow for a feedback effect of nonlinear interactions on the breathing mode at first order, which may lead to instability and chaotic oscillations in the radial motion itself.

In the present work a different mechanism is envisaged: the radial oscillation mode plays the role of transferring energy from the external pressure field to the subharmonic oscillation of one distortion mode, without being affected at leading order, while instability and chaos occur due to nonlinear interactions between distortion modes.

Experimental evidence (Benjamin & Ellis 1990) shows that two or at most three oscillation modes are dominant in the bubble shape distortion when the wave amplitude threshold values provided by linear stability theory are exceeded. The same linear theory suggests that those modes which are closer to the wave angular frequency ω or to an integral fraction of it are most likely to be excited, subharmonic oscillations being the most unstable. Thus in the present paper we perform a nonlinear stability analysis of bubble surface oscillations allowing for the interaction of two adjacent modes of the bubble shape distortion.

Following Hall & Seminara (1980) we examine the case in which the angular frequency ω of the incident wave is sufficiently close to both $2\omega_3$ and ω_4, thus exciting respectively a subharmonic oscillation of mode 3 and a synchronous one of mode 4. Using the multiple-scale perturbation method we find that these oscillations are modulated by slowly varying amplitudes, the evolution of which is governed by an autonomous system of quadratically coupled nonlinear equations, displaying both regular and chaotic solutions.

A similar system has been found by Gu & Sethna (1987) for resonant surface waves of a liquid in a rectangular container subjected to vertical oscillations under particular resonance conditions.

We discuss the behaviour of the solutions and find that, within a particular range of values of ω when the wave amplitude is increased, they undergo successive bifurcations leading, through a period-doubling sequence (*Feigenbaum scenario*), to a chaotic state. The excitation of two adjacent modes passively drives at second order the development of mode 1, the amplitude of which may also display a chaotic behaviour.

The procedure followed in the rest of the paper is as follows: in §2 we formulate the hydrodynamic problem and state the basic radial motion of the cavity; in §3 the results of linear stability analysis of shape oscillations are reviewed; in §4 a nonlinear stability analysis of two interacting modes is performed; in §5 the resulting amplitude equations are studied while in §6 numerical experiments are reported. Some conclusions follow in §7.

2. Formulation and basic radial oscillation

Let us consider a cavity immersed in a liquid filling an unbounded region characterized by an average ambient pressure P_∞^* (the asterisk denotes dimensional quantities). A permanent, non-condensable gas fills the cavity with equilibrium pressure P_0^*. (We neglect the effects of the vapour present in the cavity.) At equilibrium the bubble radius R_0 reads

$$R_0 = \frac{2\sigma}{P_0^* - P_\infty^*} \tag{2.1}$$

where σ is surface tension.

Let us now assume the liquid to be irradiated by an acoustic wave with wavelength sufficiently large compared with R_0 to be 'felt' by the bubble as an oscillation of the pressure at infinity of the form $P^*_\infty(1+\epsilon\cos\omega t^*)$ with ϵ,ω amplitude and frequency of the wave respectively and t^* time. We wish to investigate the response of the bubble to a small-amplitude acoustic excitation under the assumption that the latter be 'weak', i.e.

$$\epsilon \ll 1 . \tag{2.2}$$

The analysis will be based on the following further assumptions:

(i) the equilibrium radius R_0 will be assumed to be constant or to vary (owing to any mechanism like rectified diffusion) on a time scale much larger than the time scales involved in the instability process under investigation;

(ii) damping effects (viscous, thermal or acoustic) will be lumped into some linear damping coefficients introduced into the final amplitude equations;

(iii) motion of the gas inside the cavity will be ignored and the state of the gas will be assumed to be isothermal.

Assumption (iii) implies that the internal pressure in the cavity is uniform: this is justified if the bubble radius is small compared with the wavelength of the sound wave. Furthermore the thermal penetration depth in the liquid must be small compared with the bubble radius for the gas to behave isothermally.

The interested reader is referred to Prosperetti (1974) and Plesset & Prosperetti (1977) for a detailed discussion of the implications of assumptions (i) and (ii).

We start by assuming the flow as inviscid irrotational, hence governed by the Laplace equation for the velocity potential ϕ^* along with kinematic and dynamic conditions at the interface and the condition that the pressure at infinity be forced by the acoustic wave. An alternative equivalent formulation from the standpoint of Hamiltonian theory has been proposed by Benjamin (1987).

Let us describe the motion of the cavity by the following equation for the interface:

$$F^*(r^*,\theta,\varphi,t^*)=0, \tag{2.3}$$

with r^*,θ,φ spherical polar coordinates, and define dimensionless variables as in Hall & Seminara (1980), namely

$$t=t^*\left(\frac{P^*_\infty}{\rho R_0^2}\right)^{1/2}, \quad (F^*,r^*)=R_0(F,r), \quad p^*=P^*_\infty p, \quad \phi^*=R_0\left(\frac{P^*_\infty}{\rho}\right)^{1/2}\phi. \tag{2.4}$$

The governing differential problem for ϕ and F reduces to

$$\nabla^2\phi=0, \tag{2.5}$$

$$\left[F_{,t}-\nabla\phi\cdot\nabla F\right]_{F=0}=0, \tag{2.6}$$

$$\left[(1+2S)\frac{V(0)}{V(t)}-(1+\epsilon\cos\Omega t)-S\,\nabla\cdot\boldsymbol{n}-\phi_{,t}+\tfrac{1}{2}(\nabla\phi)^2\right]_{F=0}=0, \tag{2.7}$$

where $V(t)$ is the instantaneous volume of the deformed bubble, $\boldsymbol{n}$ is the unit vector of the local outward normal to the interface, Ω is the dimensionless form of the forcing frequency and S is the inverse of a Weber number squared. The parameters Ω and S (along with ϵ) govern the phenomenon under investigation and read:

$$\Omega=\frac{\omega R_0}{(P^*_\infty/\rho)^{1/2}}, \quad S=\frac{\sigma}{P^*_\infty R_0} . \tag{2.8}$$

Also notice that the dimensionless fluid velocity is defined here as $-\nabla\phi$.

The above system allows for the simplest flow solution in the form of a purely radial motion of the fluid driven by the interface in the form

$$\phi = \frac{R^2\dot{R}}{r}, \quad F = r - R(t) = 0\,. \tag{2.9}$$

Substituting from (2.9) into (2.5)–(2.7) the differential problem is reduced to a generalized Rayleigh equation for $R(t)$ which admits periodic solutions readily obtainable in terms of power series of the small parameter ϵ. Provided Ω does not attain a value close to an integral fraction or multiple of the natural frequency Ω_0 of the 'breathing mode' of the bubble one finds

$$R = 1 + \epsilon\rho_1(t) + O(\epsilon^2)\,, \tag{2.10}$$

where

$$\rho_1 = R_1 \cos \Omega t \tag{2.11}$$

and

$$R_1 = (\Omega^2 - \Omega_0^2)^{-1}, \tag{2.12}$$

$$\Omega_0^2 = 3 + 4S. \tag{2.13}$$

3. Linear stability of axisymmetric shape perturbations

The linear stability of the basic radial oscillatory motion (2.10), (2.11) was investigated by Benjamin & Strasberg (1958), Hsieh & Plesset (1961) and Eller & Crum (1970). We briefly recall here the main results.

Let

$$F = r - \left[R(t) + \sum_{n=0}^{\infty} f_n(t) P_n(\mu)\right], \tag{3.1}$$

$$\phi = \frac{R^2\dot{R}}{r} + \sum_{n=0}^{\infty} \phi_n(t) r^{-(n+1)} P_n(\mu) \tag{3.2}$$

be the perturbed configuration with $g_n(t)$, $\phi_n(t)$ infinitesimal amplitudes and $P_n(\mu)$ ($\mu = \cos\theta$) a Legendre polynomial of order n. Since the set of orthonormal functions $P_n(\mu)$ is complete the representation (3.1), (3.2) is suitable to describe any arbitrary infinitesimal and axisymmetric perturbation. Also notice that (3.2) satisfies the Laplace equation in spherical coordinates and the boundary condition which forces ϕ to decay as $r \to \infty$.

Requiring that the solution (3.1), (3.2) should also satisfy the linearized form of the kinematic and dynamic boundary conditions (2.6), (2.7) one ends up with the following Mathieu type equation (higher-order terms, which can be found in Hall & Seminara (1980), will not be necessary for the present analysis):

$$\frac{\mathrm{d}^2 y_n}{\mathrm{d}T^2} + [a_n + (b_n \cos 2T)\epsilon + O(\epsilon^2)]\; y_n = 0\,, \tag{3.3}$$

where

$$y_n = R^{3/2} f_n, \quad T = \tfrac{1}{2}\Omega t\,, \tag{3.4}$$

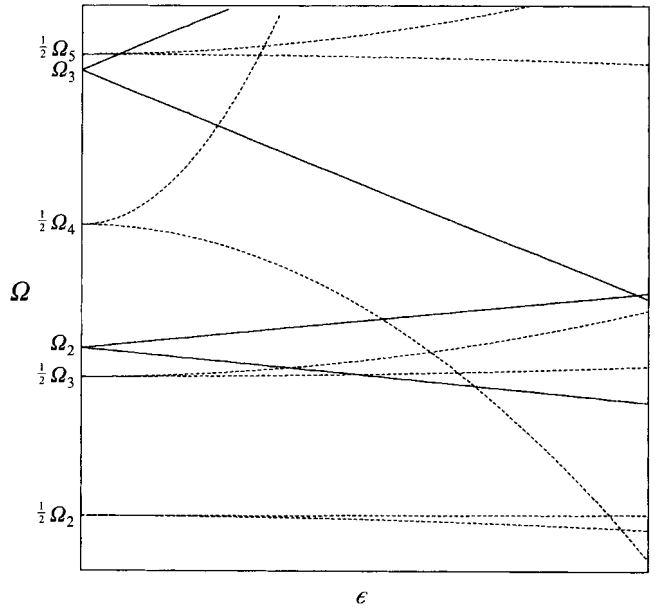

FIGURE 1. Stability chart showing critical stability curves for subharmonic (—) and synchronous (- - -) oscillations of various modes (after Hall & Seminara 1980).

$$a_n = \left(\frac{\Omega_n}{\Omega}\right)^2, \tag{3.5a}$$

$$b_n = 4R_1\left\{(n+\tfrac{1}{2}) - \tfrac{3}{4}a_n\right\}. \tag{3.5b}$$

Here Ω_n is the natural frequency of the nth mode given by

$$\Omega_n = [4S(n^2-1)(n+2)]^{1/2}. \tag{3.6}$$

The solution of (3.3) is known to be of the form

$$y_n = \exp(\sigma_n T)\Pi_n(T) \tag{3.7}$$

where σ_n is the growth rate and $\Pi_n(T)$ is a periodic function of T. A classical stability analysis for the solutions of the Mathieu equation shows that in the plane of parameters (a_n, ϵ) unstable regions (i.e. with Re $(\sigma_n) > 0$) exist in a neighbourhood of the points $(N^2, 0)$ with $N = 1, 2, \ldots$. For $N = 1$ solutions are subharmonic, for $N = 2$ synchronous and for $N > 2$ ultraharmonic.

Referring these results to the plane (ϵ, Ω) it will be clear that for any Ω sufficiently close to the natural frequency Ω_n of the nth mode the corresponding a_n will be close to unity, so that stability regions for subharmonic oscillations of each mode can be drawn in a neighbourhood of each Ω_n. The same reasoning repeated for those values of Ω which lie close to $\frac{1}{2}\Omega_n$ leads to finding stability regions for synchronous oscillations and so on. The resulting stability chart is shown in figure 1.

It should be noticed that the mode $n = 1$ is excluded since in this case the derivation of (18) ceases to be valid. This corresponds to the fact that the natural frequency of mode 1 vanishes.

Let us finally recall that for small ϵ the growth rate of subharmonic perturbations $(N = 1)$ obtained from linear theory is $O(\epsilon)$ while it is $O(\epsilon^2)$ for synchronous or ultraharmonic perturbations $(N \geqslant 2)$.

4. Nonlinear evolution of two adjacent modes

We now assume the forcing dimensionless frequency Ω to lie between Ω_3 and $\frac{1}{2}\Omega_4$:

$$\Omega = \Omega_3(1 + \lambda_3\epsilon) = \tfrac{1}{2}\Omega_4\left(1 + \tfrac{1}{2}\lambda_4\epsilon\right) , \tag{4.1}$$

with λ_3, λ_4 $O(1)$ parameters, $\lambda_3 < 0, \lambda_4 > 0$.

The choice of $n = 3$ arises from the experimental observations of Benjamin & Ellis (1990). However, the analysis would be qualitatively similar for any pair of subharmonic–synchronous modes both excited in a neighbourhood of the forced frequency Ω.

Furthermore let us take advantage of the fact, suggested by the linear theory, that subharmonic perturbations for low values of ϵ evolve both on the 'fast' time scale described by the variable T and on the 'slow' time scale described by the 'slow' variable τ defined as

$$\tau = \epsilon T . \tag{4.2}$$

Thus we set

$$\frac{\partial}{\partial t} = \frac{\Omega}{2}\left(\frac{\partial}{\partial T} + \epsilon\frac{\partial}{\partial \tau}\right) \tag{4.3}$$

and attempt to analyse the nonlinear development of the two adjacent modes 3 and 4.

Let $Z_3(\tau)$ and $Z_4(\tau)$ be the slowly varying amplitudes of modes P_3 and P_4, whose fast time dependence is respectively subharmonic (hence proportional to e^{iT}) and synchronous (hence proportional to e^{2iT}). Furthermore let ϵ^x and ϵ^y be the respective orders of magnitude of the above modes, with x and y exponents to be determined. The condition which determines the values of x and y is the requirement that secular terms arising from nonlinear interaction between the perturbations, from linear interactions of the perturbations with the basic flow and from the slow time dependence of the amplitudes Z_3 and Z_4 should vanish.

One readily finds that the spatial P_3 structure and the fast (subharmonic) time dependence of mode 3 are reproduced by:

interactions of modes 3 and 4 at order ϵ^{x+y};

interactions of mode 3 with the basic flow at order ϵ^{x+1};

slow time dependence of mode 3 at order ϵ^{x+1}.

We then require that

$$x + y = x + 1 . \tag{4.4}$$

Similarly the spatial P_4 structure and the fast (synchronous) time dependence of mode 4 are reproduced by:

interactions of mode 3 with itself at order ϵ^{2x};

slow time dependence of mode 4 at order ϵ^{y+1}.

Hence we also require that

$$2x = y + 1 . \tag{4.5}$$

From (4.4), (4.5) it then follows that

$$x = y = 1 . \tag{4.6}$$

Therefore in order to remove the occurrence of secular terms at second order, we assume the following expansions:

$$F = r - [R(t) + \epsilon f_1 + \epsilon^2 f_2 + O(\epsilon^3)] \tag{4.7}$$

with

$$f_1 = f_{31}(T,\tau)P_3 + f_{41}(T,\tau)P_4, \tag{4.8}$$

$$f_2 = f_{32}(T,\tau)P_3 + f_{42}(T,\tau)P_4 + \text{orthogonal terms}; \tag{4.9}$$

and

$$\phi = \frac{R^2\dot{R}}{r} + \epsilon\phi_1 + \epsilon^2\phi_2 + O(\epsilon^3) \tag{4.10}$$

with

$$\phi_1 = \frac{1}{r^4}\phi_{31}(T,\tau)P_3 + \frac{1}{r^5}\phi_{41}(T,\tau)P_4, \tag{4.11}$$

$$\phi_2 = \frac{1}{r^4}\phi_{32}(T,\tau)P_3 + \frac{1}{r^5}\phi_{42}(T,\tau)P_4 + \text{orthogonal terms}, \tag{4.12}$$

which we feed into the kinematic boundary condition (2.6) and the dynamic boundary condition (2.7) using (4.1), (4.2) and (4.3). Hereafter the kinematic boundary condition and the dynamic boundary condition will be referred to as KBC and DBC respectively. Notice that the notation employed above has to be read as follows: the first index refers to the order of the spatial Legendre mode while the second index identifies the order of magnitude of the perturbation.

We then perform the scalar product of (2.6)–(2.7) with P_3, P_4 and obtain the following differential problems at the various orders of approximation.

$O(\epsilon)$:

mode P_3

$$\text{KBC} \qquad \tfrac{1}{2}\Omega_2 f_{31,T} + 4\phi_{31} = 0, \tag{4.13}$$

$$\text{DBC} \qquad \tfrac{1}{2}\Omega_3\phi_{31,T} + 10Sf_{31} = 0; \tag{4.14}$$

mode P_4

$$\text{KBC} \qquad \tfrac{1}{4}\Omega_4 f_{41,T} + 5\phi_{41} = 0, \tag{4.15}$$

$$\text{DBC} \qquad \tfrac{1}{4}\Omega_4\phi_{41,T} + 18Sf_{41} = 0. \tag{4.16}$$

These systems are readily solved in the form

$$f_{31} = Z_3(\tau)\mathrm{e}^{\mathrm{i}T} + \text{c.c.}, \tag{4.17}$$

$$\phi_{31} = \tfrac{1}{8}\Omega_3\left(\mathrm{i}Z_3(\tau)\mathrm{e}^{\mathrm{i}T} + \text{c.c.},\right) \tag{4.18}$$

$$f_{41} = Z_4(\tau)\mathrm{e}^{2\mathrm{i}T} + \text{c.c.}, \tag{4.19}$$

$$\phi_{41} = \tfrac{1}{10}\Omega_4\left(\mathrm{i}Z_4(\tau)\mathrm{e}^{2\mathrm{i}T} + \text{c.c.},\right) \tag{4.20}$$

where c.c. stands for complex conjugate and Z_3, Z_4 are complex functions of the slow variable τ to be determined at higher order.

$O(\epsilon^2)$:

At this order interactions reproduce a second-order component of mode P_3 with the same fast time dependence; so does the interaction with the basic flow, as already

known by linear stability analysis. Indeed we find:

KBC

$$\tfrac{1}{2}\Omega_3 f_{32,T} - 4\phi_{32} = \left[-\tfrac{1}{2}\Omega_3\left(\mathrm{i}\lambda_3 Z_3 + \frac{\mathrm{d}Z_3}{\mathrm{d}\tau}\right) - \mathrm{i}\left(\Omega - \tfrac{5}{4}\Omega_3\right) R_1 \bar{Z}_3 + \left(\tfrac{5}{22}\Omega_3 - \tfrac{4}{11}\Omega_4\right)\mathrm{i}\bar{Z}_3 Z_4\right] \mathrm{e}^{\mathrm{i}T} + \mathrm{NST}, \tag{4.21}$$

DBC

$$\tfrac{1}{2}\Omega_3\phi_{32,T} + 10 S f_{32} = \left[\tfrac{1}{16}\Omega_3^2\left(\lambda_3 Z_3 - \mathrm{i}\frac{\mathrm{d}Z_3}{\mathrm{d}\tau}\right) + \left(10S - \tfrac{1}{2}\Omega^2 - \tfrac{1}{8}\Omega_3^2 + \tfrac{1}{4}\Omega\Omega_3\right) R_1 \bar{Z}_3 + \tfrac{2}{11}\left(60S - \tfrac{1}{4}\Omega_4^2 - \tfrac{1}{4}\Omega_3^2 + \tfrac{3}{8}\Omega_3\Omega_4\right)\bar{Z}_3 Z_4\right] \mathrm{e}^{\mathrm{i}T} + \mathrm{NST}, \tag{4.22}$$

where NST stands for non-secular terms.

From (4.21), (4.22) a differential equation for f_{32} follows:

$$f_{32,TT} + f_{32} = \left[2\lambda_3 Z_3 - 2\mathrm{i}\frac{\mathrm{d}Z_3}{\mathrm{d}\tau} + \tfrac{11}{2} R_1 \bar{Z}_3 + \tfrac{2}{11}\left(-\tfrac{1}{2} + 10\frac{\Omega_4}{\Omega_3} - 4\frac{\Omega_4^2}{\Omega_3^2}\right)\bar{Z}_3 Z_4\right] \mathrm{e}^{\mathrm{i}T} + \mathrm{NST}. \tag{4.23}$$

The suppression of secular terms requires that the following amplitude equation be satisfied:

$$\frac{\mathrm{d}Z_3}{\mathrm{d}\tau} = -\mathrm{i}\lambda_3 Z_3 - \mathrm{i}\tfrac{11}{4} R_1 \bar{Z}_3 - \mathrm{i}\tfrac{1}{2}\bar{Z}_3 Z_4. \tag{4.24}$$

Similarly interactions reproduce a second-order P_4 component with a synchronous time dependence. We find:

KBC

$$\tfrac{1}{2}\Omega_4 f_{42,T} - 5\phi_{42} = \left[-\tfrac{1}{4}\Omega_4\left(\mathrm{i}\lambda_4 Z_4 + \frac{\mathrm{d}Z_4}{\mathrm{d}\tau}\right) - \tfrac{81}{154}\mathrm{i}Z_3^2 +\right] \mathrm{e}^{2\mathrm{i}T} + \mathrm{NST}, \tag{4.25}$$

DBC

$$\tfrac{1}{4}\Omega_4\phi_{42,T} + 18 S f_{41} = \left[\frac{\Omega_4^2}{40}\left(\lambda_4 Z_4 + \mathrm{i}\frac{\mathrm{d}Z_4}{\mathrm{d}\tau}\right) + \tfrac{18}{77}\left(22S - \tfrac{25}{64}\Omega_3^2\right)\bar{Z}_3^2\right] \mathrm{e}^{\mathrm{i}T} + \mathrm{NST}. \tag{4.26}$$

Proceeding as before it follows that

$$f_{42,TT} + 4 f_{42} = \left[4\lambda_4 Z_4 - 4\mathrm{i}\frac{\mathrm{d}Z_4}{\mathrm{d}\tau} + \tfrac{18}{77}\left(18\frac{\Omega_3}{\Omega_4} + \tfrac{44}{9} - \tfrac{125}{4}\frac{\Omega_3^2}{\Omega_4^2}\right) Z_3^2\right] \mathrm{e}^{2\mathrm{i}T} + \mathrm{NST}. \tag{4.27}$$

Removal of secular terms then leads to a second amplitude equation in the form

$$\frac{\mathrm{d}Z_4}{\mathrm{d}\tau} = -\mathrm{i}\lambda_4 Z_4 - \mathrm{i}\tfrac{27}{154} Z_3^2 . \tag{4.28}$$

So far we have neglected the effect of viscosity and assumed the liquid motion to be inviscid irrotational. Indeed in the case of shape oscillations the neglect of viscous effects is justified only if the thickness of the Stokes boundary layer over the bubble surface, namely $\delta^* = (2\nu/\omega)^{1/2}$ (ν being kinematic viscosity), is much smaller than the bubble radius (Lamb 1932, Arts. 352-3; Longuet-Higgins 1989*b*, §4).

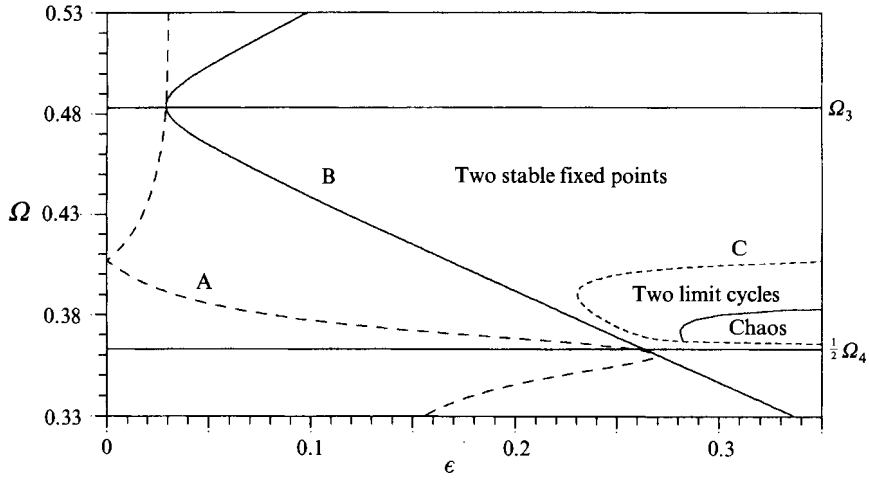

FIGURE 2. Different stability regions corresponding to parameter values as specified in §5.

The effect of viscosity is a weak dissipation of energy, which we take into account by introducing in the amplitude equations suitable linear damping terms, whose coefficients are given in the form suggested by Lamb (1932, n. 355) for free oscillations, namely

$$\beta_n^* = (2n+1)(n+2)\frac{\nu}{R_0^2}. \tag{4.29}$$

The dimensionless boundary layer thickness defined as

$$\delta = \frac{\delta^*}{R_0}\,. \tag{4.30}$$

will be assumed to scale in the form

$$\delta = \alpha(\epsilon)\epsilon \tag{4.31}$$

with $\alpha \sim O(1)$. As a consequence the effect of viscosity will be incorporated in the amplitude equations (4.21), (4.25) by means of linear damping terms whose coefficients will be

$$\beta_n = (2n+1)(n+2)\alpha\,. \tag{4.32}$$

In the present case ($n = 3$) we have respectively

$$\beta_3 = 35\alpha\,, \quad \beta_4 = 54\alpha\,. \tag{4.33a, b}$$

5. Amplitude equations

The system of equations governing the slow variation of the amplitudes of modes P_3 and P_4 finally reads

$$\frac{dZ_3}{d\tau} = -\,i\lambda_3 Z_3 + i\mu_3\bar{Z}_3 - \beta_3 Z_3 - i\kappa_3\bar{Z}_3 Z_4\,, \tag{5.1}$$

$$\frac{dZ_4}{d\tau} = -\,i\lambda_4 Z_4 - \beta_4 Z_4 - i\kappa_4 Z_3^2\,, \tag{5.2}$$

where $\mu_3 = \frac{11}{4}R_1, \kappa_3 = \frac{1}{2}, \kappa_4 = \frac{27}{154}$.

Let us introduce for convenience the following rescaled variables:

$$z_3 = (\kappa_3\kappa_4)^{1/2} Z_3, \qquad z_4 = \kappa_3 Z_4 \,. \tag{5.3}$$

Then the system becomes

$$\frac{\mathrm{d}z_3}{\mathrm{d}\tau} = -(\mathrm{i}\lambda_3 + \beta_3)z_3 + \mathrm{i}\mu_3\bar{z}_3 - \mathrm{i}\bar{z}_3 z_4 \,, \tag{5.4}$$

$$\frac{\mathrm{d}z_4}{\mathrm{d}\tau} = -(\mathrm{i}\lambda_4 + \beta_4)z_4 - \mathrm{i}z_3^2 \,. \tag{5.5}$$

Notice that the above system can be reduced, by means of suitable parameter and variable transformations, to that found by Gu & Sethna (1987). The discussion of the solutions of (5.4), (5.5) depends on the nature of the coefficients and their dependence on the physical parameters governing the phenomenon under examination. Such a discussion is given below and reveals some interesting features.

5.1. *Fixed points*

Fixed points of the above differential system are solutions of the algebraic system

$$(\mathrm{i}\lambda_3 + \beta_3)z_3 - \mathrm{i}\mu_3\bar{z}_3 + \mathrm{i}\bar{z}_3 z_4 = 0 \,, \tag{5.6}$$

$$(\mathrm{i}\lambda_4 + \beta_4)z_4 + \mathrm{i}z_3^2 = 0 \,. \tag{5.7}$$

The latter is invariant under substitution of z_3 with $-z_3$. This implies that fixed points always occur in couples having the same values for z_4 and opposite values for z_3.

The origin is always a fixed point. Then let us look for non-trivial solutions. From (5.7) we have at once

$$z_4 = -\frac{\lambda_4 + \mathrm{i}\beta_4}{\lambda_4^2 + \beta_4^2} z_3^2 \,. \tag{5.8}$$

Substituting into (5.6) and writing for convenience $z_3 = r_3 \exp(\mathrm{i}\vartheta_3)$, the former can be split into

$$r_3^4 + 2(\beta_3\beta_4 - \lambda_3\lambda_4)r_3^2 + (\lambda_3^2 + \beta_3^2 - \mu_3^2)(\beta_4^2 + \lambda_4^2) = 0 \,, \tag{5.9}$$

$$\sin(2\vartheta_3) = \frac{1}{\mu_3}\left(\beta_3(\beta_4^2 + \lambda_4^2) + \beta_4 r_3^2\right) \,, \tag{5.10}$$

$$\cos(2\vartheta_3) = \frac{1}{\mu_3}\left(\lambda_3(\beta_4^2 + \lambda_4^2) - \lambda_4 r_3^2\right) \,. \tag{5.11}$$

An inspection of coefficients shows that (5.9) admits at most one positive solution provided the following conditions are simultaneously fulfilled:

$$\mu_3^2 - \frac{(\lambda_3\beta_4 + \lambda_4\beta_3)^2}{(\lambda_4^2 + \beta_4^2)} \geqslant 0 \,, \tag{5.12}$$

$$\lambda_3^2 + \beta_3^2 - \mu_3^2 < 0 \,. \tag{5.13}$$

The former condition is satisfied for all points lying on the right of curve A in figure 2, while the latter holds for all points on the right of curve B. Notice that this curve corresponds to the marginal stability curve of linear theory when a weak viscous damping is included.

To each solution of (5.9) however two distinct values for ϑ_3 correspond, both satisfying (5.10), (5.11) and differing by π, as expected due to the already noted symmetry.

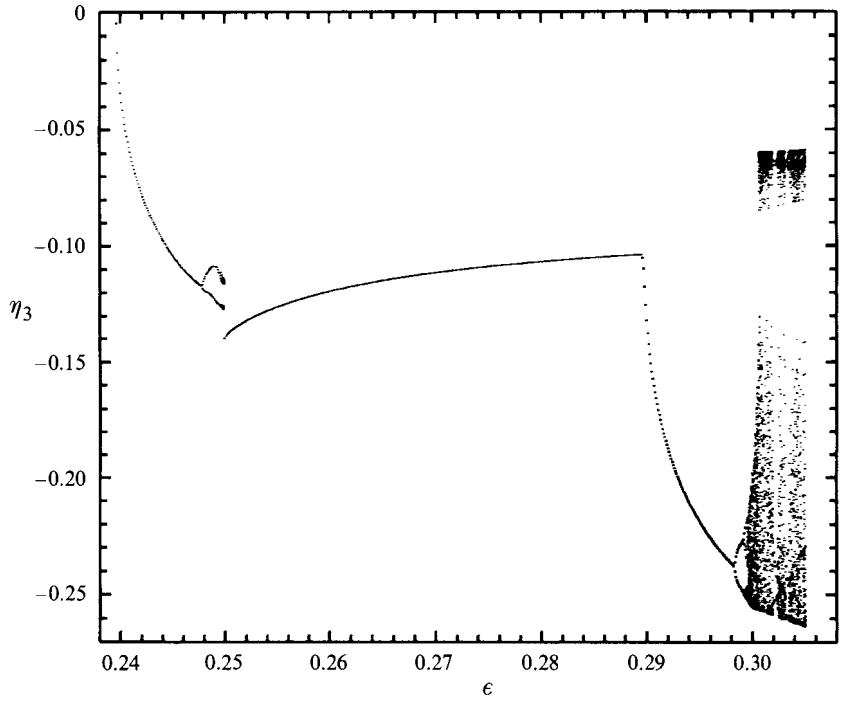

FIGURE 3. Bifurcation diagram.

When (5.12)–(5.13) are satisfied the solution of (5.9) reads

$$r_3 = \left(\lambda_3\lambda_4 - \beta_3\beta_4 + \left(\mu_3^2(\lambda_4^2 + \beta_4^2) - (\lambda_3\beta_4 + \lambda_4\beta_3)^2\right)^{1/2}\right)^{1/2} . \tag{5.14}$$

Then we obtain from substitution into (5.10)–(5.11) two values for ϑ_3:

$$\vartheta_{31} = \frac{1}{2}\arctan\left(\frac{\beta_3(\beta_4^2 + \lambda_4^2) + \beta_4 r_3^2}{\lambda_3(\beta_4^2 + \lambda_4^2) - \lambda_4 r_3^2}\right) , \tag{5.15}$$

$$\vartheta_{32} = \vartheta_{31} + \pi . \tag{5.16}$$

The (unique) corresponding value for z_4 is given by (5.8).

5.2. *Stability of fixed points*

The characteristic polynomial evaluated in an arbitrary point $z_3 = x_3 + \mathrm{i}y_3, z_4 = x_4 + \mathrm{i}y_4$ reads

$$\begin{aligned} P(\lambda) = {} & \left[(\beta_4 + \lambda)^2 + \lambda_4^2\right]\left[-y_4^2 + (\beta_3 + \lambda)^2 + \lambda_3^2 - (x_4 + \mu_3)^2\right] \\ & + 4(x_3^2 + y_3^2)\left[(\beta_4 + \lambda)(\beta_3 + \lambda) - \lambda_3\lambda_4\right] + 4(x_3^2 + y_3^2)^2 . \end{aligned} \tag{5.17}$$

When the point is the origin, the roots are readily found and read

$$\lambda^{(1)} = -\beta_3 + \left(\lambda_3^2 - \mu_3^2\right)^{1/2} , \quad \lambda^{(2)} = -\beta_3 - \left(\lambda_3^2 - \mu_3^2\right)^{1/2} , \tag{5.18a, b}$$

$$\lambda^{(3)} = -\beta_4 + i\lambda_4 , \quad \lambda^{(4)} = -\beta_4 - \mathrm{i}\lambda_4 . \tag{5.18c, d}$$

We conclude that the origin is always a stable fixed point – a sink ($\lambda_4 \neq 0$) or an inflected node ($\lambda_4 = 0$) – for the mode 4, while it may be unstable with respect to the mode 3 if $|\lambda_3|$ exceeds μ_3 by a sufficiently large amount that gives $\lambda^{(1)} > 0$.

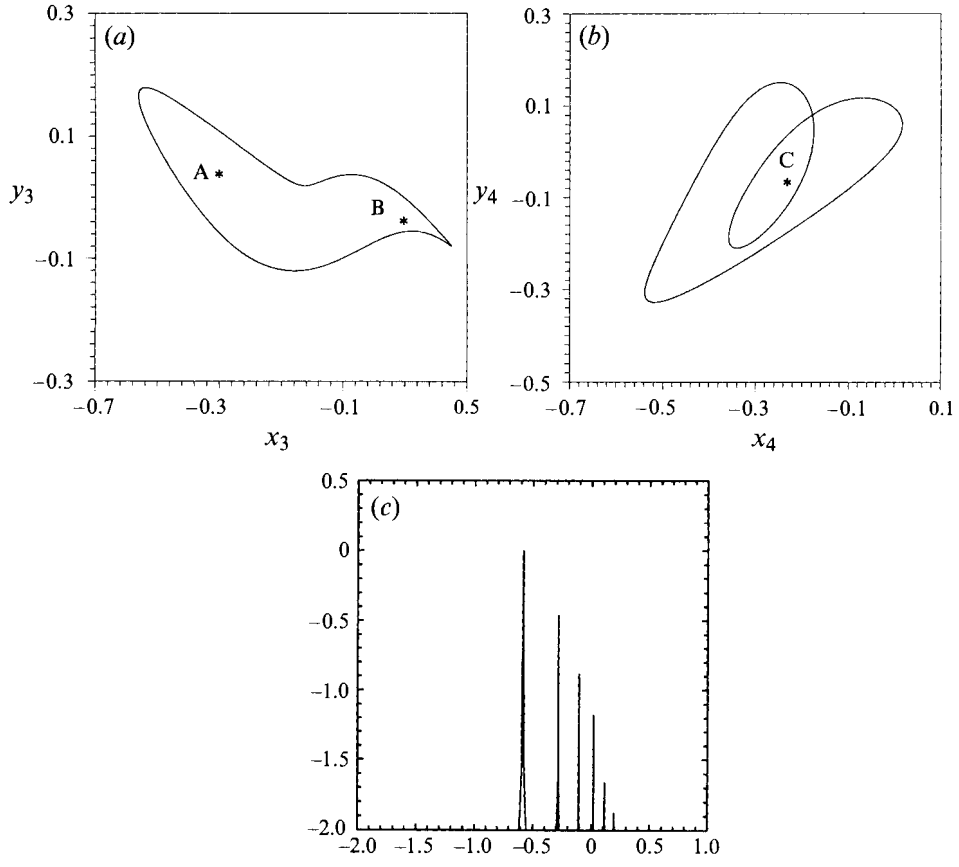

FIGURE 4. Two-sided limit cycle at $\epsilon = 0.2950$. (*a*) Projection over the (x_3, y_3)-plane; (*b*) projection over the (x_4, y_4)-plane; (*c*) power spectrum of $x_3(t)$.

When non-trivial fixed points exist, rather than finding explicitly the corresponding eigenvalues we are interested in determining their signs, which are provided by the Routh–Hurwitz criterion (Pearson 1983, p. 254).

The characteristic polynomial may be written in the form

$$P(\lambda) = J_4\lambda^4 + J_3\lambda^3 + J_2\lambda^2 + J_1\lambda + J_0 \tag{5.19}$$

where

$$J_4 = 1\,, \quad J_3 = 2(\beta_3 + \beta_4)\,, \quad J_2 = \beta_4^2 + \lambda_4^2 + 4(r_3^2 + \beta_3\beta_4)\,, \tag{5.20a–c}$$

$$J_1 = 2\beta_3(\beta_4^2 + \lambda_4^2) + 4r_3^2(\beta_3 + \beta_4)\,, \quad J_0 = 4r_3^2\left[\beta_3\beta_4 - \lambda_3\lambda_4 + r_3^2\right]\,. \tag{5.20d, e}$$

According to the above criterion, the fixed points are stable if the following inequalities hold:

$$J_0 > 0\,, \quad J_1 > 0\,, \quad J_3J_4 > 0\,, \tag{5.21a–c}$$

$$J_1\,(J_2J_3 - J_1J_4) - J_0J_3^2 > 0\,. \tag{5.21d}$$

While conditions (5.21*a–c*) are always fulfilled, (5.21*d*) holds only for particular values

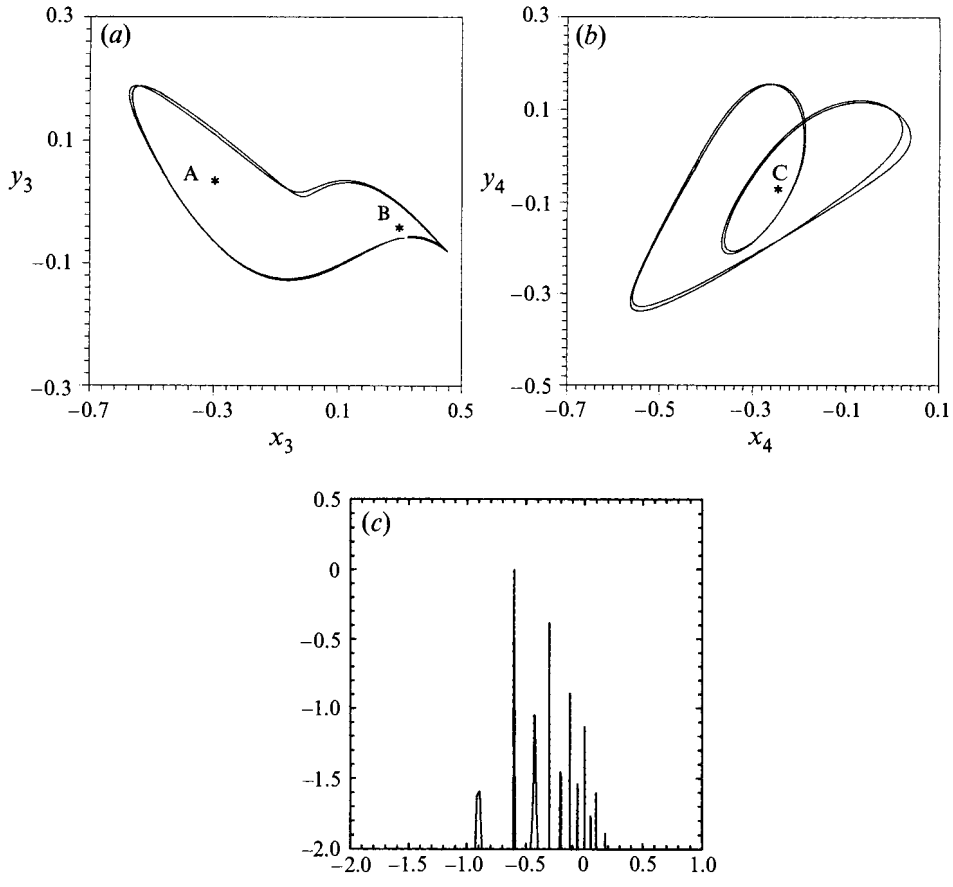

FIGURE 5. Double orbit at $\epsilon = 0.2990$.

of the parameters. Substituting from (5.20*a–e*), condition (5.21*d*) can be written

$$(\lambda_4^2+\beta_4^2)\left(\frac{\beta_4}{\beta_3}(\lambda_4^2+\beta_4^2)+4\beta_4(\beta_3+\beta_4)\right)+2\left(1+\frac{\beta_4}{\beta_3}\right)^2 r_3^2(\lambda_4^2+\beta_4^2+2\beta_3\beta_4+2\lambda_3\lambda_4)>0\,. \tag{5.22}$$

Notice that the first term is always positive; therefore the above condition is not satisfied only if

$$\lambda_4^2+\beta_4^2+2\beta_3\beta_4+2\lambda_3\lambda_4<0\,. \tag{5.23}$$

The region on the right of curve C in figure 2 corresponds to points at which (5.21*d*) is not verified: when the characteristic parameters of the system are varied so that the representative point on the (ϵ,Ω)-plane crosses the curve from left to right, the fixed point undergoes a Hopf bifurcation and two symmetric limit cycles appear.

6. Numerical experiments

In order to explore the behaviour of solutions of the system (5.4)–(5.5) a large number of numerical experiments was performed employing a fourth-order Runge–Kutta method. We have detected the occurrence of various successive bifurcations of the solutions as the wave amplitude ϵ was increased with Ω lying in the range of wave frequencies for which a Hopf bifurcation has been seen to take place.

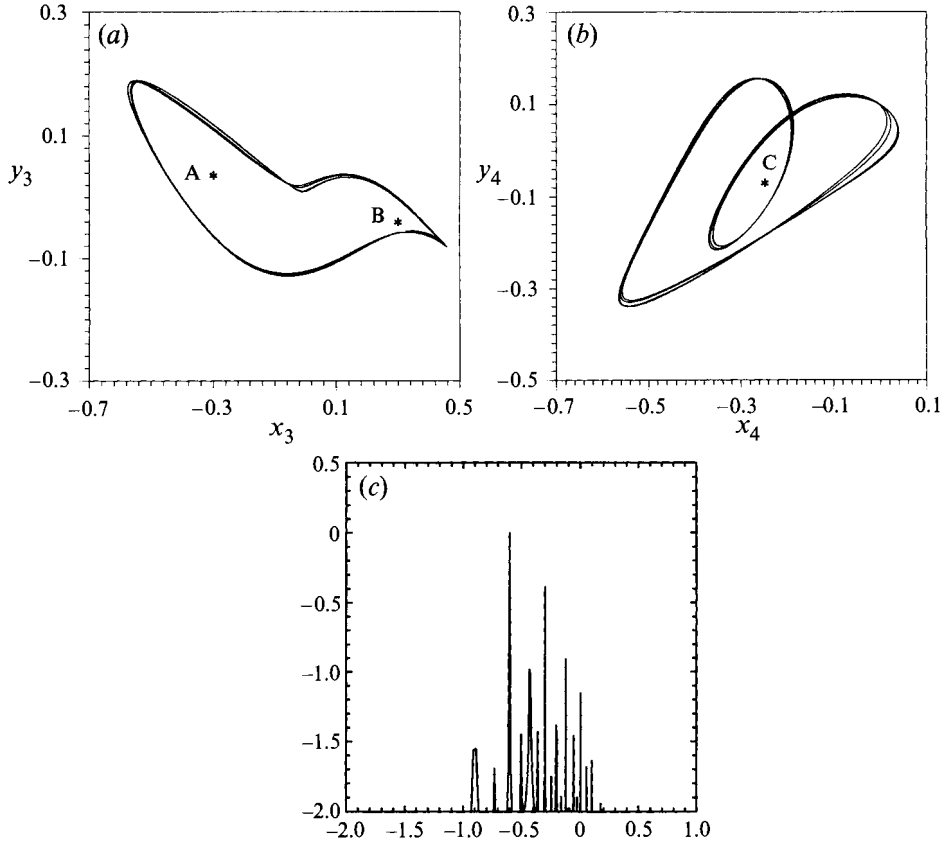

FIGURE 6. Quadruple orbit at $\epsilon = 0.2993$.

In the following we summarize the typical results obtained when considering the case of helium bubbles in water (cf. Benjamin & Ellis 1990) with typical equilibrium radius $R_0 = 0.5$ mm. We have assumed the following parameter values: surface tension $\sigma = 0.074$ N m^{-1}, water density $\rho = 998$ kg m^{-3}, viscosity $\nu = 10^{-6}$ m^2 s^{-1}, ambient pressure $P_\infty^* = 101325$ Pa, at 20°C. We fix the wave frequency at $\omega = 7.660$ kHz corresponding to $\Omega = 0.38$.

In order to follow the bifurcation pattern as ϵ is varied, we have plotted a bifurcation diagram obtained through successive Poincaré sections (Parker & Chua 1989). To this purpose it seemed convenient to introduce the following change of variables, consisting of a rotation and rescaling over the (x_3, y_3)-plane and a translation over the (x_4, y_4)-plane:

$$\xi_3 = \frac{1}{r_3}(x_3 \cos\vartheta_3 + y_3 \sin\vartheta_3)\,, \quad \eta_3 = \frac{1}{r_3}(-x_3 \sin\vartheta_3 + y_3 \cos\vartheta_3) \qquad (6.1a, b)$$

$$\xi_4 = x_4 - \frac{r_3^2}{\lambda_4^2 + \beta_4^2}(\lambda_4 \cos 2\vartheta_3 - \beta_4 \sin 2\vartheta_3)\,, \qquad (6.1c)$$

$$\eta_4 = y_4 - \frac{r_3^2}{\lambda_4^2 + \beta_4^2}(\lambda_4 \sin 2\vartheta_3 + \beta_4 \cos 2\vartheta_3)\,. \qquad (6.1d)$$

This choice was aimed at eliminating the rotation of fixed points, and hence also of

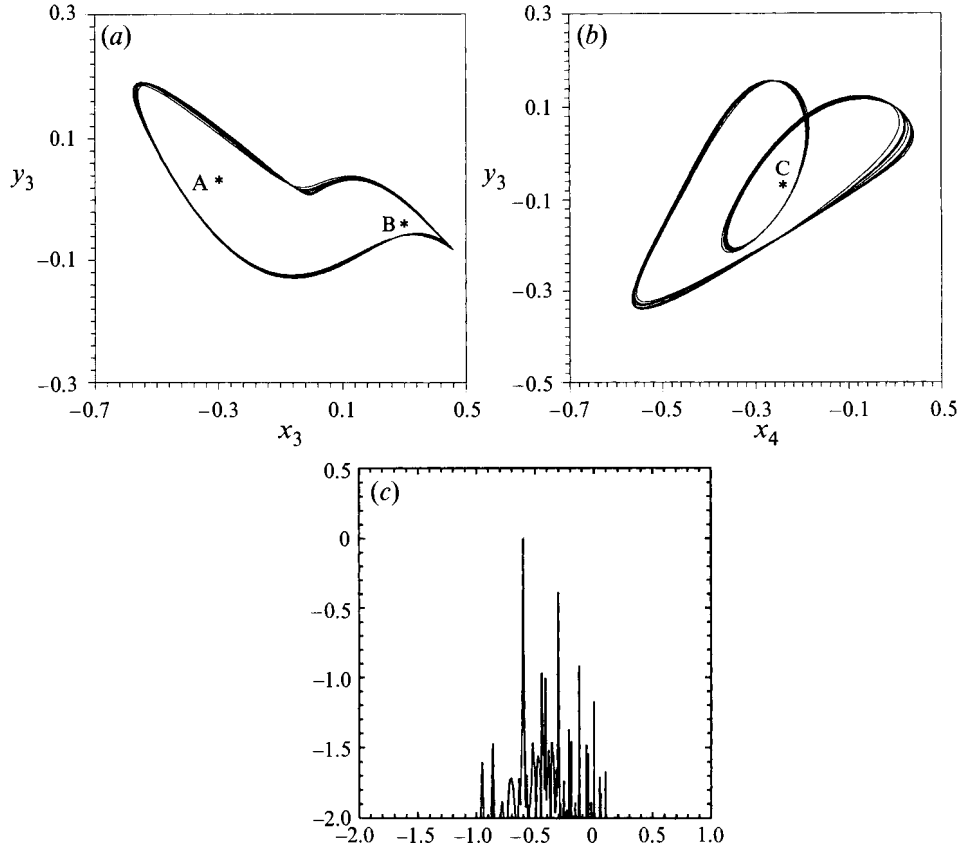

FIGURE 7. Chaos at $\epsilon = 0.2997$.

the outcoming attractor, when ϵ is varied: in the new coordinates the fixed points are always (-1,0,0,0) and (1,0,0,0), so that in this 'intrinsic' frame of reference only the relative shape of the attractor is changed as the wave amplitude is increased.

We have chosen as intersection surface for Poincaré sections the hyperplane $\xi_3 = 1$. Then for each value of ϵ we have recorded the second coordinate of the points at which the orbit intersects the plane, after the transient had died out, for a consistent number of periods. The resulting diagram is shown in figure 3. The first bifurcation from a stable fixed point to a limit cycle occurs at $\epsilon = (0.23995 \pm 0.00005)$ as given by (5.21*d*) (figure 4). As ϵ is increased, the mean radius of the cycle increases. At $\epsilon = (0.24775 \pm 0.00005)$ an incomplete bifurcation sequence takes place (Thompson & Stewart 1986, p. 172). At $\epsilon = (0.28955 \pm 0.00005)$ a saddle-node bifurcation occurs, with the appearance of an unstable orbit. At $\epsilon = \epsilon_1 \equiv (0.29829 \pm 0.00005)$ a first period doubling occurs (figure 5) followed by a second one at $\epsilon = \epsilon_2 \equiv (0.29917 \pm 0.00001)$ (figure 6), a third one at $\epsilon = \epsilon_3 \equiv (0.2993575 \pm 0.0000005)$ and so on until a chaotic state is reached (figure 7).

Figure 8 shows an enlargement of a bifurcation diagram from which it is possible to see in more detail the succession of period doublings. The values of ϵ at which bifurcations occur satisfy fairly well the Feigenbaum criterion, namely:

$$\lim_{n\to\infty} r_n \equiv \lim_{n\to\infty} \frac{\epsilon_{n-1} - \epsilon_{n-2}}{\epsilon_n - \epsilon_{n-1}} = 4.6692016\ldots$$

as shown in table 1.

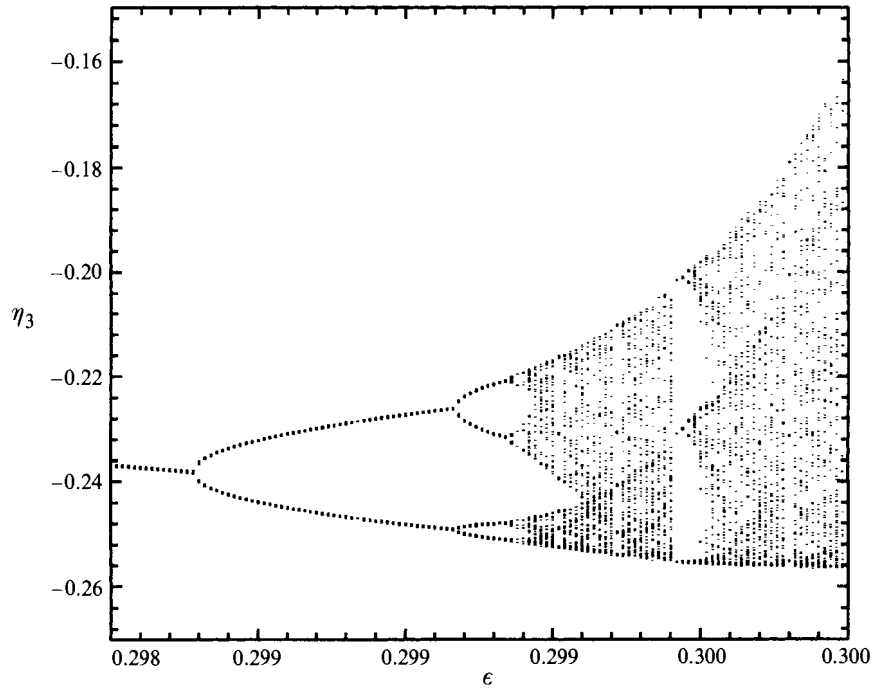

FIGURE 8. Enlarged details of Feigenbaum scenario.

n	ϵ_n	$\Delta\epsilon_n$	$\epsilon_n - \epsilon_{n-1}$	r_n
1	0.2982900	10^{-5}	-	-
2	0.2991700	10^{-5}	$0.0008800 \pm 2.5\%$	-
3	0.2993575	5×10^{-7}	$0.0001900 \pm 5.5\%$	$4.63 \pm 8\%$
4	0.2993980	5×10^{-7}	$0.0000405 \pm 2.5\%$	$4.69 \pm 8\%$

TABLE 1.

We also computed the correlation dimension d of the outcoming strange attractor, defined as (Moon 1987, p. 216):

$$d = \lim_{r \to 0} \frac{\log C(r)}{\log r}$$

where

$$C(r) = \lim_{N \to \infty} \frac{1}{N^2} \left\{ \begin{array}{c} \text{number of points over the attractor} \\ \text{such that their distance apart is smaller than } r \end{array} \right\},$$

N being the total number of points of the attractor considered.

The resulting value for the dimension of the final chaotic attractor turns out to be

$$d = 1.58\,,$$

which was obtained as usual (Parker & Chua 1989, p. 188) by evaluating the slope of the plot of $\log C$ versus $\log r$ in its middle range (figure 9).

According to Benjamin & Ellis (1990) the velocity of the bubble centroid along the

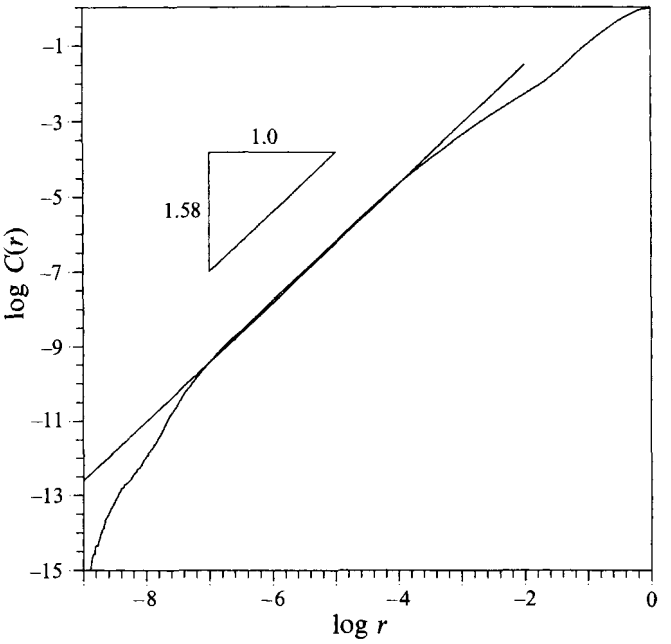

FIGURE 9. Log-log plot of the correlation function $C(r)$ of the attractor ($\epsilon = 0.2997$). The slope of the curve in the linear middle part gives the required correlation dimension of the attractor.

axis of symmetry is given, in dimensional form, by

$$W^* = \omega R_0 \sum_{n=2}^{\infty} \frac{9}{2n+3} \dot{f}_n f_{n+1} \epsilon^2 + O(\epsilon^3) , \tag{6.2}$$

which in the present case reduces to

$$W^* = \omega R_0 \dot{f}_3 f_4 \epsilon^2 + O(\epsilon^3) . \tag{6.3}$$

Substituting from (4.14)–(4.16) we therefore obtain

$$W^* = \tfrac{1}{2}\Omega \left[\mathrm{i} Z_3 Z_4 e^{3\mathrm{i}T} - \mathrm{i} \bar{Z}_3 Z_4 \mathrm{e}^{\mathrm{i}T} + \text{c.c.} \right] \omega R_0 \epsilon^2 + O(\epsilon^3) . \tag{6.4}$$

The time dependence of the centroid velocity in the range where chaos occurs is plotted in figure 10.

7. Conclusions

The mechanism envisaged herein appears to confirm that Benjamin & Ellis' (1990) suggestion can indeed explain the origin of the *'erratic drift'* phenomenon. However, one should be aware that a variety of similar but distinct mechanisms may operate as the frequency and amplitude of the acoustic excitation are varied. They encompass two-mode interactions of the subharmonic–subharmonic or of synchronous–synchronous type which lead to amplitude equations with cubic coupling. An attempt at such analysis was made by Norris (1991). As ϵ increases one may reasonably expect the involvement of an increasing number of modes in the interaction process. A complete understanding of the phenomenon does indeed require a full numerical solution of the problem, a task which we are at present undertaking. The interesting question we would like to answer is to what extent, in the present process, chaos is

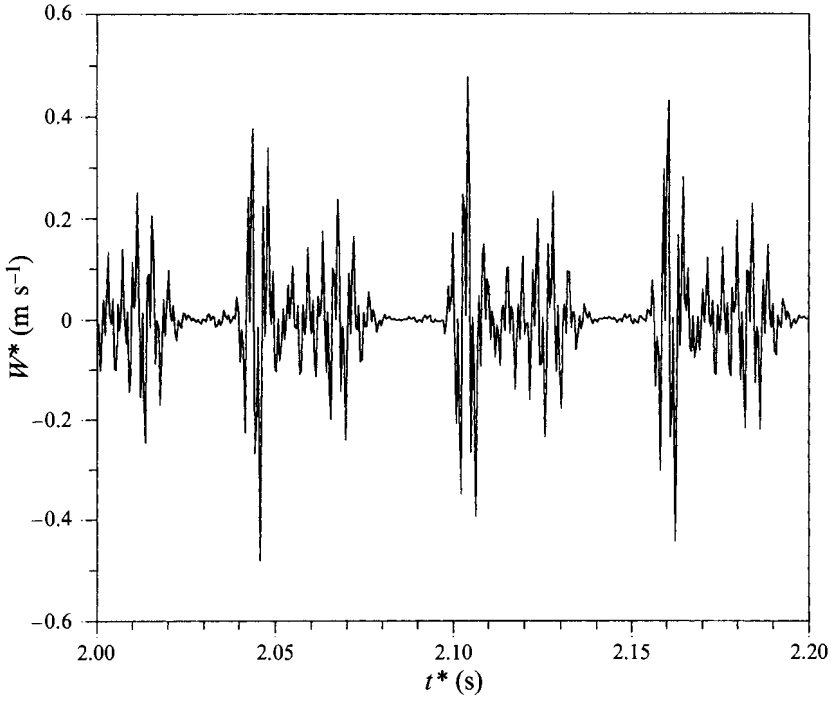

FIGURE 10. Bubble centroid velocity in the range where chaos occurs (parameter values are the same as in figure 7).

dependent on the low-dimensional nature of the problem that we generate when we restrict ourselves to weakly nonlinear conditions.

Further some unexplained aspects of the process still await an answer. In particular the role of viscous effects for large-amplitude shape oscillations does not appear to have received attention either in the axially symmetric (bubble) or in the plane (Faraday resonance) case.

To what extent the experimental observations, which concern the behaviour of bubbles within a mixture, may be interpreted by considering the response of an isolated bubble subject to acoustic excitation is also a fairly open subject which will require attention in the near future.

This work is part of the junior author's (D. Z.) thesis to be submitted to the University of Genoa in partial fulfillment of the requirements for the PhD degree in Hydrodynamics.

The authors wish to acknowledge Professor L. Van Wijngaarden and Professor W. Lauterborn for providing useful references on topics related to that discsussed in the present paper.

REFERENCES

BENJAMIN, T. B. 1987 Hamiltonian theory for motions of bubbles in an infinite liquid. *J. Fluid Mech.* **181**, 349–379.

BENJAMIN, T. B. & ELLIS, A. T. 1990 Self-propulsion of asymmetrically vibrating bubbles. *J. Fluid Mech.* **212**, 65–80.

BENJAMIN, T. B. & STRASBERG, M. 1958 Excitation of oscillations in the shape of pulsating gas bubbles; Theoretical work. (Abstract) *J. Acoust. Soc. Am.* **30**, 697.

CILIBERTO, S. & GOLLUB, J. P. 1985 Chaotic mode competition in parametrically forced surface waves. *J. Fluid Mech.* **158**, 381–398.

ELDER, S. A. 1959 Cavitation microstreaming *J. Acoust. Soc. Am.* **31**, 54–64

ELLER, A. I. & CRUM, L. A. 1970 Instability of the motion of a pulsating bubble in a sound field. *J. Acoust. Soc. Am.* **47**, 762–767.

FENG, Z. C. & LEAL, L. G. 1994 Bifurcation and chaos in shape and volume oscillations of a periodically driven bubble with two-to-one internal resonance *J. Fluid Mech.* **266**, 209–242.

FENG, Z. C. & SETHNA, P. R. 1989 Symmetry-breaking bifurcation in resonant surface waves. *J. Fluid Mech.* **199**, 495–518.

GAINES, N. 1932 Magnetostriction oscillator producing intense audible sound and some effects obtained. *Physics* **3**, 209–229.

GOULD, R. K. 1966 Heat transfers across a solid–liquid interface in the presence of acoustic streaming. *J. Acoust. Soc. Am.* **40**, 219–225.

GU, X. M. & SETHNA, P. R. 1987 Resonant surface waves and chaotic phenomena. *J. Fluid Mech.* **183**, 543–565.

HALL, P. & SEMINARA, G. 1980 Nonlinear oscillations of non-spherical cavitation bubbles in acoustic fields. *J. Fluid Mech.* **101**, 423–444.

HOLMES, P. 1986 Chaotic motions in a weakly nonlinear model for surface waves. *J. Fluid Mech.* **162**, 365–388.

HSIEH, D. Y. & PLESSET, M. S. 1961 Theory of rectified diffusion of mass into gas bubbles. *J. Acoust. Soc. Am.* **33**, 206–215.

KAMBE, T. & UMEKI, M. 1990 Nonlinear dynamics of two-mode interactions in parametric excitation of surface waves. *J. Fluid Mech.* **212**, 373–393.

KORNFELD, M. & SUVOROV, L. 1944 On the destructive action of cavitation. *J. Appl. Phys.* **15**, 495–506.

LAMB, H. 1932 *Hydrodynamics*, 6th edn. Cambridge University Press.

LONGUET-HIGGINS, M. S. 1989*a* Monopole emission of sound by asymmetric bubble oscillations. Part 1. Normal modes *J. Fluid Mech.* **201**, 525–541.

LONGUET-HIGGINS, M. S. 1989*b* Monopole emission of sound by asymmetric bubble oscillations. Part 2. An initial-value problem *J. Fluid Mech.* **201**, 543–565.

MEI, C. C. & ZHOU, X. 1991 Parametric resonance of a spherical bubble *J. Fluid Mech.* **229**, 29–50.

MILES, J. W. 1984 Nonlinear Faraday resonance. *J. Fluid Mech.* **146**, 285–302.

MOON, F. C. 1987 *Chaotic Vibrations.* John Wiley & Sons.

NORRIS, J. W. 1991 Abstract presented at First European Fluid Mechanics Conference, Cambridge.

PARKER, T. S. & CHUA, L. O. 1989 *Practical Numerical Algorithms for Chaotic Systems.* Springer-Verlag.

PEARSON, C. E. 1983 *Handbook of Applied Mathematics.* Van Nostrand Reinhold Company.

PLESSET, M. S. & MITCHELL, T. P. 1956 On the stability of the spherical shape of a vapor cavity in a liquid *Q. Appl. Maths* **13**, 419–430.

PLESSET, M. S. & PROSPERETTI, A. 1977 Bubble dynamics and cavitation. *Ann. Rev. Fluid Mech.* **9**, 145–185.

PROSPERETTI, A. 1974 Nonlinear oscillation of gas bubbles in liquids: steady state solutions. *J. Acoust. Soc. Am.* **56**, 878–885.

RALSTON, A. & WILF, H. S. 1960 *Mathematical methods for digital computers*, vol. 1. John Wiley & Sons.

RAYLEIGH, LORD 1917 On the pressure developed in a liquid during the collapse of a spherical cavity. *Phil. Mag.* **34**, 94–98.

SAFFMAN, P. G. 1967 The self-propulsion of a deformable body in a perfect fluid. *J. Fluid Mech.* **28**, 385–389.

SIMONELLI, F. & GOLLUB, J. P. 1989 Surface wave mode interactions: effects of symmetry and degeneracy. *J. Fluid Mech.* **199**, 471–494.

STRASBERG, M. & BENJAMIN, T. B. 1958 Excitation of oscillations in the shape of pulsating gas bubbles; Experimental work. (Abstract) *J. Acoust. Soc. Am.* **30**, 697.

THOMPSON, J. M. T. & STEWART, H. B. 1986 *Nonlinear Dynamics and Chaos.* John Wiley & Sons.